Effect of Soft Filler Particles on Polymer Diffusion in Poly(butyl methacrylate) Latex Films

Ewa Odrobina, Jianrong Feng,† Hung H. Pham,‡ and Mitchell A. Winnik*

Department of Chemistry, University of Toronto, 80 St. George St., Toronto, Ontario, Canada M5S 3H6

Received December 1, 2000; Revised Manuscript Received May 11, 2001

ABSTRACT: We examine the influence of small (56 nm diameter) cross-linked poly(butyl acrylate) (xPBA) particles as fillers on the diffusion rate of poly(butyl methacrylate) (PBMA) molecules in PBMA latex films. For the high-*M* PBMA sample (M_w = 400 000), the presence of soft, elastic particles strongly decreases the diffusion rate of the PBMA molecules across the intercellular boundaries. The retardation effect increases linearly with xPBA content, with the surface-to-volume ratio for xPBA particles of different size, and is best explained as an obstacle effect on the PBMA diffusion rate. For the low-*M* PBMA sample (M_w = 35 000), the presence of 30 vol % cross-linked PBA particles increases the diffusion rate of the PBMA polymer, whereas in the presence of 60 vol % cross-linked PBA particles, the PBMA diffusion rate is the same as that in the latex film without filler. Thus, the overall effect of soft filler particles on polymer diffusion is a combination of an obstacle effect, which retards polymer diffusion, and a second effect, probably a free volume effect, which promotes polymer diffusion. This effect is much smaller for the high-*M* PBMA sample. Depending on which of these effects dominates, one can observe an increase or decrease in the polymer diffusion rate.

Introduction

Additives affect the final properties of latex films. Some additives like plasticizers dissolve in the latex polymer. Other additives form separate domains (occlusions) within the film. The effect of hard fillers on the mechanical properties of polymers[1] and on polymer diffusion[2] has been explored extensively. The addition of hard fillers to elastomers can increase the strength and hardness of the material and its resistance to deformation. These particles also act to retard polymer diffusion. We know much less about how "soft" filler particles influence the dynamic properties of latex films. In this paper we show that cross-linked elastomeric filler particles in poly(butyl methacrylate) (PBMA) latex films can either enhance or retard the rate of polymer diffusion. These effects depend on the molecular weight of the PBMA polymer and are also connected to the presence of the PBMA polymer adjacent to the surface of the soft filler particles. To put our work in context, we begin with a review of the influence of surfaces on the dynamics of an adjacent polymer phase.

The change in the properties of polymer films in the presence of fillers is, to some extent, connected with the fact that polymer chains near a filler surface have substantially different properties than those in the bulk.[3−5] This is due to chain conformational changes attributed to the presence of a boundary, and specific interactions between the polymer and the interface, which, in certain cases, can propagate away from the surface up to $50R_g$[6] or even "tie" portions of the chain to the interface. In addition, geometry effects can play a role. The filler particles can act as obstacles to increase the diffusion path of the polymer (a tortuosity effect). Ensembles of these particles can create channels with a diameter smaller than the mean dimensions of the polymer molecules in the matrix. This situation creates a barrier for the diffusion of polymer molecules through the restricted space between the filler particles: the diffusion of the polymer chain through this space proceeds by overcoming the entropic bottlenecks generated by the random media.[6]

Most studies of polymer diffusion near a solid substrate have indicated a reduction in polymer mobility close to the substrate.[7−9] For example, Zheng et al.[8] found from dynamic scanning ion mass spectrometry measurements that the diffusion rates of polystyrene (PS) perpendicular to a silicon oxide substrate were as much as an order of magnitude slower than in bulk even up to 80 nm ($10R_g$ from the surface). Frank et al.[7] found smaller, but substantial, decreases in lateral polymer diffusion coefficients in PS films with thicknesses up to 150 nm ($50R_g$) cast on a silicon oxide substrate. In substrate-supported poly(methyl methacrylate) (PMMA) films, Lin et al.[9] found that the range of influence of silicon oxide on polymer diffusion away from the surface was at most 40 nm ($4R_g$). These results have been interpreted in terms of a decrease in polymer mobility associated with an increase in the effective T_g of the polymer molecules near the surface. Others, however, have reported an enhancement in polymer mobility in the presence of a solid surface, and a decrease in T_g was also observed[10−12] in similar systems. Both Orts et al.[10] and Keddie et al.[11] observed that ultrathin polystyrene films on silicon oxide surfaces (with a weakly attractive interaction energy) exhibit a lower glass transition temperature than the bulk polymer. Additionally, Reiter[12] observed that polystyrene films dewetted silicon oxide surfaces at temperatures below the bulk polymer T_g, providing evidence of enhanced chain mobility.

In contrast, the air−polymer interface is often thought of as a region of enhanced mobility. Brillouin scattering studies of freely standing, ultrathin polystyrene films

* To whom correspondence should be addressed: e-mail mwinnik@chem.utoronto.ca.

† Permanent address: Thompson Gordon Ltd., 325 Mainway, Burlington, ON, Canada L7M 1A6.

‡ Permanent address: Polymer Coating Technologies of Singapore Pte Ltd., 16 Joo Koon Crescent, Singapore 629018.

10.1021/ma002052e CCC: $20.00
Published on Web 07/18/2001

by Dutcher and co-workers[13,14] indicated substantial reductions in T_g as thickness is reduced. Simulations indicate that this free surface region may have decreased density compared to the bulk.[4] It has also been argued that chain-end segregation to a surface due to conformational entropy considerations may increase the local free volume and thus increase polymer mobility.[6] In summary, polymer surfaces have a significant influence on polymer mobility in the regions of the polymer close to the surface.

Long and Lequeue[15] argue that the changes in polymer density close to the surface for freely suspended or strongly adsorbed films are not sufficient to cause measurable changes in the T_g. To explain the shift in the glass transition temperature of thin films compared to the same polymer in the bulk, they introduced a new model, based upon thermally induced density fluctuations in the polymer, in which the distribution of these fluctuations is responsible for the T_g shift. The authors estimate the size of the fluctuations to be on the order of 1 nm. Above T_g, there are small regions of high density within the bulk, which according to the free volume theory will have low mobility. The volume fraction of these domains is small, and they do not percolate. Below T_g, the volume fraction of the domains with slow dynamics is high enough for percolation to occur. When percolation takes place, the sample becomes macroscopically rigid. The threshold for percolation is higher in two dimensions than in three dimensions. As a consequence, polymer adjacent to a free surface or a weakly interacting interface will remain mobile at temperatures where a thick polymer film will be rigid. On the other hand, domains of high density are attracted to the interface for a strongly adsorbed polymer. This effect reduces the mobility of the polymer in the layer adjacent to a strongly interacting interface. Thin films, where this effect dominates, are in the glassy state for temperatures at which the bulk polymer is in a fluid state, so the T_g of the strongly adsorbed films is increased in comparison to that of the bulk polymer.

In our studies of polymer diffusion in latex films, we have begun to examine the influence of hard particles (e.g., silica, PMMA latex) as fillers. While one might imagine that there are strong interactions with the silica surface and weak interactions with the PMMA particle surface, both additives retard the rate of polymer diffusion in the film-forming polymer. In this context, we became interested in the influence of weakly interacting soft surfaces on the mobility of polymer molecules in an adjacent phase. We were specifically interested in what type of effect one would obtain if one prepared a latex film containing a second component consisting of soft cross-linked nanospheres. These types of blends can be prepared from a mixed aqueous dispersion of two types of latex particles: one latex that will form the continuous phase in the latex film formed when the dispersion dries and cross-linked low-T_g particles with a different chemical composition. If the cross-link density is sufficiently large, the second component will resist coalescence, deformation, and molecular level mixing with the other component in the blend.

In this paper we examine the rate of polymer diffusion in films prepared from a mixture of poly(butyl methacrylate) (PBMA) latex particles containing linear polymer and cross-linked poly(butyl acrylate) (xPBA) particles. We use a fluorescence technique based upon direct nonradiative energy transfer (DET) to follow the diffusion of PBMA molecules in these films. The PBMA component of these films consists of a mixture of nearly identical particles: half labeled with phenanthrene (Phe) as the donor chromophores and half labeled with anthracene (An) as the acceptor. Our objective is to examine the influence of the xPBA as a soft filler material on the rate of polymer diffusion. For the 100 nm diameter PBMA component, we investigate the influence of polymer chain length by considering two samples of very different molecular weight. For the xPBA component, we consider particle size and blend composition as the major variables. In all of the dispersions we employ, the particles have a very narrow size distribution.

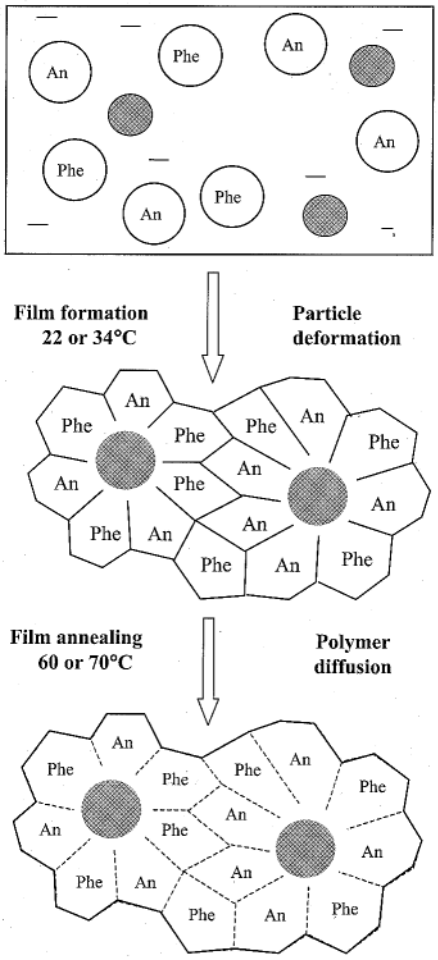

Figure 1. Schematic representation of the formation and annealing processes for a film prepared from a blend of PBMA (1:1 Phe- + An-labeled) and cross-linked xPBA filler particles.

In Figure 1 we present a schematic description of the formation of films from this mixture of latex particles. In the aqueous phase the particles are spherical. Upon drying, the PBMA particles deform to a transparent film made up of polyhedral cells. In the drawing, Phe and An refer to the nature of the label in each cell. The xPBA filler is shown as darker gray spheres, where we imagine that the relatively high cross-link density provides sufficient elasticity for the particle to remain spherical. We will see that this picture of the structure of the filler particles may not always be correct.

Experimental Section

Materials. *Latex Samples.* Poly(butyl methacrylate) (PBMA) latex particles labeled with a fluorescence dye (either a donor,

Table 1. Characteristics of the PBMA Latex Samples

	M_w (g/mol)	M_n (g/mol)	d (nm)	T_g (°C)	dye content (mol %)
high M					
Phe−PBMA	380 000	130 000	124	34	0.9
An−PBMA	420 000	130 000	132	34	0.9
low M					
Phe−PBMA	35 000	16 000	120	21	0.9
An−PBMA	34 000	17 000	120	21	1

Table 2. Recipe for the Preparation of Cross-Linked xPBA Latex

first stage (56 nm cross-linked xPBA seeds)		second stage (112 nm cross-linked xPBA)	
BA (mL)	16.062	BA (mL)	10.657
cross-linker[a] (g)	0.626	cross-linker (g)	0.387
KPS[b] (g)	0.358	KPS (g)	0.06
SDS[c] (g)	1.154	SDS (g)	0.4
water (g)	372	water (mL)	28
temp (°C)	80	temp (°C)	80
time (h)	1	time (h)	3

[a] 1,6-Hexanediol diacrylate. [b] KPS = potassium persulfate; [c] SDS = sodium dodecyl sulfate.

phenanthrene (Phe), or an acceptor, anthracene (An), referred to as Phe−PBMA and An−PBMA, respectively) were prepared by standard semicontinuous emulsion polymerization techniques as described previously.[16,17] We prepared both high (high M) and low (low M) molecular weight particles at 30 wt % solids at 80 °C, using potassium persulfate as the initiator and *n*-dodecyl mercaptan as the chain-transfer agent (for the low-M latex). All the latex samples have a narrow particle size distribution, as indicated by dynamic light scattering. Some important characteristics of the PBMA latex particles are present in Table 1. Feng[16] showed previously that PBMA with M_w 35 000 and $M_w/M_n = 2$ has a glass transition temperature (T_g) nearly 15 °C lower than that of high molecular weight PBMA.

Fluorescent-dye-labeled latex particles were employed both in direct energy transfer (DET) and in modulated differential scanning calorimetry (MDSC) experiments. In the case of the MDSC measurements, we used the labeled polymer to ensure that we used the same samples for both types of experiments.

Filler Particles. Two samples of unlabeled fully cross-linked poly(butyl acrylate) (xPBA) latex particles with $T_g = -43$ °C and diameters $d = 56$ and 112 nm were prepared by conventional emulsion polymerization using the recipes presented in Table 2. The 56 nm xPBA latex was obtained by batch polymerization. Part of this sample was used as the seed in the semicontinuous polymerization used to prepare the 112 nm diameter xPBA latex. In both reactions, 3.75 wt % of 1.6-hexanediol diacrylate (HDA) was added as the cross-linker.

From the data in Table 2 and the density of the BA monomer ($\rho = 0.894$ g/cm^3), we calculated M_c, the mean molecular weight between cross-links, to be 2600 (20 BA units), assuming that both $H_2C{=}CHCO_2$ groups of HDA react. We assume 100% gel content for these particles. For the $d = 56$ nm xPBA latex, some attempts were made to measure the gel content. A xPBA film prepared at room temperature was transferred to a centrifuge tube filled with tetrahydrofuran (THF) as the solvent. The film was left for 24 h in the solvent for swelling. Under these conditions the film fell apart. The xPBA fragments coming from the latex film redispersed in THF and the cloudy solution obtained could not be sedimented by normal centrifugation. Nevertheless, we assume that the xPBA latex particles are fully cross-linked. These xPBA latex particles were used as a soft fillers in the preparation of PBMA latex films.

Sample Preparation. All the dispersions, including PBMA and xPBA, were cleaned by ion exchange three times (Bio-Rad, AG-501-X8 mixed bed resin, 3 g resin per 100 mL of latex) to remove the ionic surfactant (sodium dodecyl sulfate) and low molecular weight salts before film formation. For both diffusion and MDSC measurements, latex films were prepared in the same way from a mixed dispersion containing a 1:1 number ratio of Phe- and An-labeled PBMA particles and a varying volume fraction of soft cross-linked PBA particles. The volume ratios in blends were calculated on the basis of the weights of solids of the various types of particles, using density values of 1.05 g/mL for PBMA and 1.08 g/mL for cross-linked PBA. The mixtures of latex dispersions were gently shaken for 10 min and then cast onto quartz (diffusion measurements) or glass slides (MDSC measurements). The plates were covered with an inverted Petri dish and placed in an oven for about 4 h to form dry, crack-free, and transparent films. Films with a higher content of xPBA (30 or 60 wt %) were slightly cloudy. The film formation temperature was 34 °C for the high-M PBMA samples and 22 °C for the low-M PBMA. After the films were dry, films on glass were cut from the glass substrate and placed in the DSC pan (in the form of small pieces), whereas films for diffusion measurements (DET) were left on their quartz plates and annealed at 55 °C (low-M PBMA) or at 70 and 80 °C (high-M PBMA). The thickness of the films was in the range 30−50 μm.

Modulated Differential Scanning Calorimetry (MDSC) Measurements. The glass transition temperature T_g of the homopolymers and their blends were determined by MDSC measurements using a Universal VI.6I TA DSC instrument. The samples were run under N_2 with a 2 °C/min average heating and cooling rate. The modulations had an amplitude of ±1 °C every 60 s. For most samples three scans were performed: scan 1 (heating from −125 to 75 °C); scan 2 (cooling from 75 to −125 °C); scan 3 (reheating from −125 to 75 °C). The total measurement required about 7 h. The T_g values were obtained as the maximum in the heat capacity derivative curves.

Fluorescence Decay Measurements. All fluorescence decay profiles were measured by the time-correlated single-photon counting technique[18] at room temperature. The donor phenanthrene was excited at 296 nm, and its emission was recorded at 350−360 nm. A band-pass filter (320−390 nm) was mounted in the front of phototube detector to minimize the scattered light and interferences due to the fluorescence from directly excited acceptors. For fluorescence decay measurements, samples were placed in small quartz test tubes and kept under a nitrogen atmosphere. In the case of annealed samples, before each measurement, they were removed from the oven and cooled to room temperatures. Then the fluorescence decay profiles were measured, and the areas under each decay curve were integrated and analyzed as described below.

Analysis of Fluorescence Decay Data

Energy-Transfer Efficiency. The rate of direct, nonradiative, energy transfer (DET) from an excited donor to an acceptor depends sensitively on the distance r between the centers of their transition dipoles.

$$w(r) = \kappa^2/\tau_D(R_0/r)^6 \tag{1}$$

In this expression, τ_D is the unquenched donor lifetime, κ^2 is the orientation parameter, and R_0 is the characteristic (Förster) energy transfer distance. For the Phe and An chromophores we employ, in PBMA films, $R_0 = 23$ Å.[19]

A useful measure of the extent of energy transfer (ET) is the quantum efficiency Φ_{ET}, which we calculate from the donor fluorescence decay profiles $I_D(t')$ for films in the presence and absence of acceptor.

$$\Phi_{ET} = 1 - \frac{\int_0^\infty I_D(t')\,dt'}{\int_0^\infty I_D{}^0(t')\,dt'} = 1 - \frac{\text{Area}(t)}{\text{Area}([An] = 0)} \tag{2}$$

The middle term represents the definition of the energy

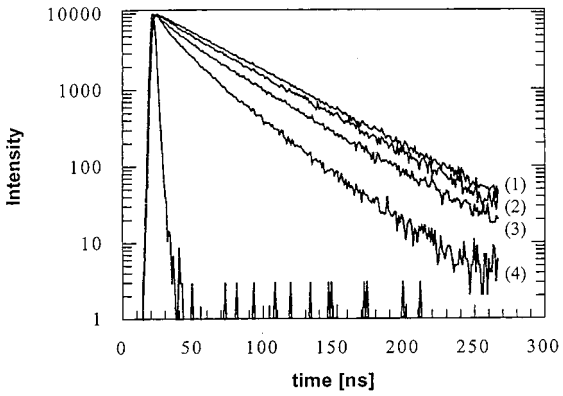

Figure 2. Donor fluorescence decay profiles for latex films annealed at 80 °C: (1) containing only phenanthrene (Phe) as a fluorescent dye; (2) for a freshly formed film containing Phe as the donor and An as the acceptor with a ratio of Phe/An = 1:1; (3) for the same film like in (2) but annealed at 80 °C for 4 h; (4) for the same film as in (2) but fully mixed.

transfer efficiency in terms of the integrated intensity decays profiles, where $I_D^0(t')$ is the donor decay profile in the absence of acceptor. For latex films containing phenanthrene as the donor, $I_D^0(t')$ is always exponential. Area(t) represents the integrated area under the fluorescence decay profile of a latex film sample annealed for a time t, and Area([An] = 0) refers to the area under the decay profile of a film containing only donor. To calculate these areas, nonexponential decay profiles are fitted to the stretched exponential (3) and then integrated analytically.

$$I_D(t') = B_1 \exp\left[-\frac{t'}{\tau_D} - P\left(\frac{t'}{\tau_D}\right)^{1/2}\right] + B_2 \exp\left(-\frac{t'}{\tau_D}\right) \quad (3)$$

The fitting parameters B_1, B_2, and P in eq 3 obtained from each profile are useful for area integration, but their physical meaning is not important here. These integrated areas have dimensions of time and define an average decay time $\langle\tau_D\rangle$ for the sample.

Polymer Diffusion in Latex Films. The PBMA latex films examined here containing only Phe as a fluorescent label exhibit an exponential fluorescence decay with a lifetime τ_D of 45.7 ns. Latex films prepared from a mixture of Phe- and An-labeled PBMA latex exhibit nonexponential donor fluorescence decay profiles that can be fitted to eq 3. Sample fluorescence decays for a freshly formed film and for an annealed PBMA film are presented in Figure 2. In freshly prepared films cast just above the minimum film forming temperature (MFT), little interdiffusion occurs, and the changes observed in the donor fluorescence decay profile $I_D(t')$ are due primarily to energy transfer across the interparticle boundary.

Polymer diffusion across the intercellular boundaries in the film leads to mixing of donor- and acceptor-labeled polymer and to an increase in Φ_{ET}. The extent of mixing upon annealing the sample, expressed in terms of the fractional growth of DET efficiency, $f_m(t)$, corrects for transboundary DET in the freshly formed film.

$$f_m \equiv \frac{\Phi_{ET}(t) - \Phi_{ET}(0)}{\Phi_{ET}(\infty) - \Phi_{ET}(0)} = \frac{\text{Area}(0) - \text{Area}(t)}{\text{Area}(0) - \text{Area}(\infty)} \quad (4)$$

where $[\Phi_{ET}(t) - \Phi_{ET}(0)]$ represents the change in DET efficiency between the initially prepared film and that aged for time t, while the term $[\Phi_{ET}(\infty) - \Phi_{ET}(0)]$ represents the change in DET efficiency between the fully mixed film and the initially prepared film. Combining the definition of DET efficiency (eq 2) with eq 4, the extent of mixing parameter f_m can be directly calculated by comparing the areas under the decays profiles for films annealed for various times [Area(t)] to that of a film without annealing [Area(0)] and to one annealed for a sufficiently long time to approach the minimum value of the area [full mixing, Area(∞)].

Our data analysis implicitly assumes that there is no significant PBMA diffusion into fully cross-linked PBA particles. This assumption is confirmed by our measurements of Area(∞), which show only small differences between pure PBMA samples and samples containing 60% vol of xPBA. We know from the work of Briber et al.[20] that even linear homopolymers and cross-linked polymers of the same composition will phase separate if the mesh size of the cross-linked polymer is less than the radius of gyration R_G of the linear polymer. Thus, we expect very little mixing of the PBMA and cross-linked PBA components. The volume of the PBMA phase and the final dye concentrations should not change substantially when soft particles are present.

The term f_m is an important parameter for characterizing the extent of polymer diffusion in latex films. Simulations show that, for the acceptor concentrations employed here and for diffusion that satisfies Fick's laws, the fraction of diffusing substance (mass fraction of mixing) f_s is proportional to f_m for f_m values up to ca. 0.7.[21] The dependence of f_m on annealing time t is discussed in detail in our previous publication.[22] Here we want to emphasize that plots of f_m vs $t^{1/2}$ are linear for our low-M polymer samples, in agreement with Fickian diffusion. For our high molecular weight samples, we observe a linear dependence of f_m on $t^{1/4}$. We believe that the $t^{1/4}$ dependence of f_m is a consequence of polymer reptation in polydisperse systems.[21]

The other fundamental parameter characterizing the rate of polymer diffusion across the latex particle interface is the diffusion coefficient. It can be calculated at different levels of rigor and sophistication.[23,24] In our case, apparent diffusion coefficients D_{app} were calculated from f_m, assuming that $f_m = f_s$, where f_s is the fraction of mass that has diffused across the initial boundary and fitting the data to a spherical Fickian diffusion model.[25] The strengths and weaknesses of this analysis have been discussed previously.[26] These apparent mean diffusion coefficients D_{app} represent an average over the broad polymer molecular weight distribution of the sample. Since the magnitude of D_{app} also represents an integration over the sample history, values of D_{app} from different samples can be compared only at similar values of f_m. The importance of these numbers is that, for samples with similar degrees of acceptor labeling, changes in D_{app}, compared at similar f_m values, correspond to changes in the true center-of-mass diffusion coefficients of the polymers.[21] However, in the case of high molecular weight polymer, the calculations of D_{app} do not take into account reptation effects.

Results

Initial Energy Transfer in Nascent Films. We begin by examining the efficiency of energy transfer in newly formed low molecular weight films $\Phi_{ET}(0)$, which provides a measure of the interfacial area between donor and acceptor labeled particles. We wanted to see whether the presence of soft fillers changes the interfacial area

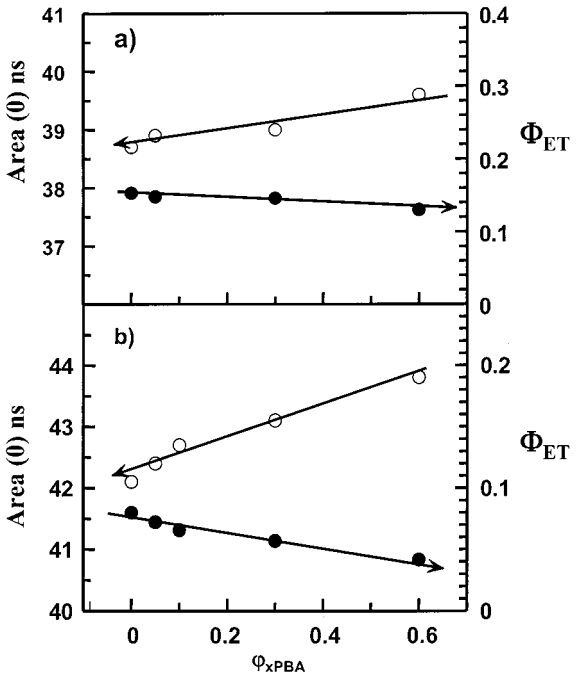

Figure 3. Plots of Area(0) (unfilled symbols) and efficiency of energy transfer ET (filled symbols) vs the soft particle volume fraction, φ_{xPBA}: (a) for low molecular weight PBMA films, (b) for high molecular weight PBMA films.

between the donor- and acceptor-labeled particles. Our results are shown in Figure 3a. We find that the amount of ET for samples with low-*M* PBMA is almost independent of the soft-particle fraction from 0 to 0.6, with the Area(0) value ranging from 38.7 to 39.6 ns, corresponding to $\Phi_{ET}(0)$ varying from 0.15 to 0.13. In the case of the high-*M* PBMA films with soft xPBA particles, we observe an increase of Area(0) and a decrease of Φ_{ET} with an increasing volume fraction of soft filler. For this system the value of Area(0) increases monotonically, on average, from 42 ns for the PBMA sample itself to 43.8 ns for the PBMA sample containing 60% xPBA, corresponding to a decrease in Φ_{ET} from 0.08 to 0.04 (see Figure 3b). These changes are small, but they are calculated by integrating the area under the decay curve. The precision of the calculation is normally better than 1%.

The Area(0) values for the samples with 60% of xPBA exhibited significant scatter and ranged for similar samples from 43 to 45 ns. When these samples were heated briefly (e.g., 7 min at 70 °C) and cooled to room temperature, the Area(0) values relax from 45 to 43 ns. In contrast, under the same annealing conditions, we did not observe any changes in the initial area of 42.4 ns for sample with 10 vol % xPBA.

When these films are annealed at higher temperature, polymer diffusion across the interparticle boundary leads to a large growth in energy transfer. In the analysis of the diffusion data, eq 4, we need to choose a value for Area(0). For the low-*M* polymer and for the high-*M* polymer with relatively small amounts of soft filler, this choice is straightforward. For the high-*M* polymer with 60% of xPBA, we choose Area(0) = 43.5 ns, with the understanding that this is the value that best describes the system after the relaxation of system.

Maximum Energy Transfer in Well-Mixed Films. To examine whether the filler particles are able to suppress diffusion for some fraction of the polymer, we examined the effect of long annealing times on the extent of polymer diffusion. We measured the extent of energy transfer for films of different blend compositions annealed for sufficiently long times that the ET values approached their maximum value $\Phi_{ET}(\infty)$. At this point, the system approaches its equilibrium state in which all the Phe- and An-labeled molecules are well mixed. In the case of low-*M* PBMA samples, annealing the films at relatively low temperatures (60 °C) for modest lengths of times, ranging from 1 to 2 days, led to fully mixed films. In high-*M* PBMA samples, where the polymer diffusion is much slower, we employed a different procedure to obtain well-mixed films. In this case, we placed a few drops of an organic solvent (tetrahydrofuran, THF) on top of the freshly formed PBMA\xPBA film to swell the film and promote mixing. After solvent evaporation, we measured the fluorescence decay of each dried film.

In both cases, for low- and high-*M* PBMA plus xPBA, the Area(∞) values for the blends are slightly higher than that for pure PBMA itself. These differences are rather small, with the area values ranging from 15.9 ns (pure PBMA) to 17.5 ns (60 vol % xPBA) and Φ_{ET} values ranging from 0.67 to 0.62 for low-*M* PBMA films. For high-*M* PBMA films, the Area(∞) values change from 17.6 ns (pure PBMA) to 19.3 ns (60 vol % xPBA) and Φ_{ET} values from 0.61 to 0.58. We conclude that all the above samples undergo sufficient interdiffusion to reach close to their full-mixing state.

The small differences in the Area(∞) and $\Phi_{ET}(\infty)$ values in the well-mixed films are not considered to be significant in our data analysis, and they do not interfere with our comparison of diffusion rates for the different samples examined here. A possible explanation for the higher value of Area(∞) for samples with large amounts of xPBA filler in comparison to the pure PBMA film is the mixing of tiny fraction of Phe-labeled PBMA segments with xPBA at the interference between these components. Phe groups in a xPBA-rich phase would have a lower probability of energy transfer than those in the PBMA phase.

PBMA Diffusion for Low-*M* PBMA Films Containing xPBA Particles. In this section, we describe the results obtained for experiments with low-*M* PBMA films containing 0, 30, and 60 vol % xPBA particles. The films were annealed at 55 °C. The results are presented in Figure 4, where we plot (a) the extent of mixing f_m vs the square root of the annealing time $t^{1/2}$ and (b) the apparent diffusion coefficient D_{app} vs f_m for the pure PBMA sample and for samples with different amounts of xPBA filler. We see that 30 vol % xPBA promotes polymer diffusion, while 60 vol % of xPBA has a negligible effect on the PBMA diffusion rate. The results are very different than those obtained for the same low-*M* PBMA in the presence of hard fillers.[2] They are also very different from those obtained for the high-*M* PBMA latex films in the presence of soft fillers, to be described below.

Since the presence of soft filler particles increases the diffusion rate of low-*M* PBMA, we carried out modulated differential scanning calorimetry (MDSC) measurements on the blends, to see whether the xPBA particles influence the glass transition temperature of the PBMA phase. For the low-*M* PBMA films, we investigated the same blend compositions as for the polymer diffusion experiments and plot the first-derivative curves in Figure 5. The upper plot shows the heating scan (from −125 to 75 °C) for films with 30 and 60 vol % xPBA

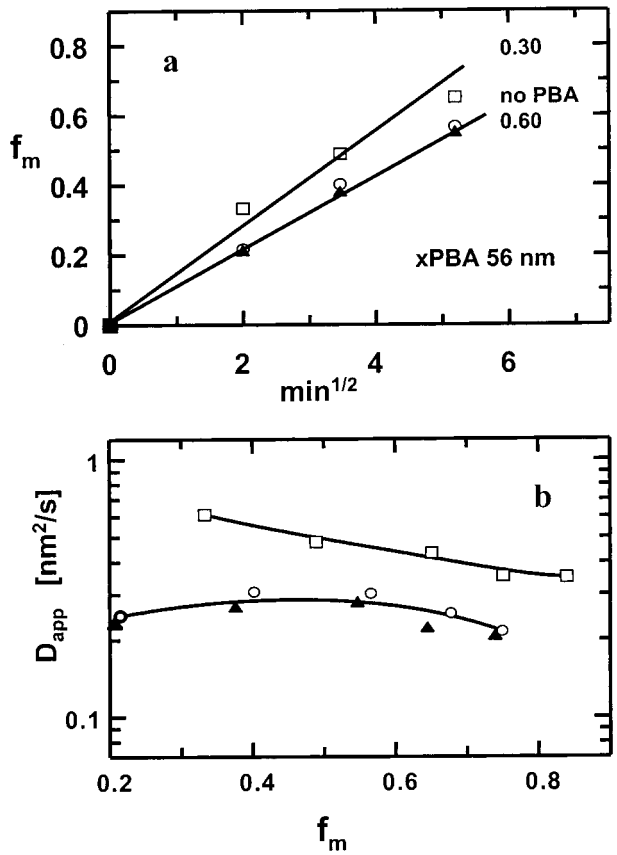

Figure 4. Comparison of diffusion rates for low-*M* PBMA latex films containing different amounts of xPBA particles (d_{xPBA} = 56 nm), expressed as volume fraction xPBA: 0 (○), 0.3 (□), and 0.6 (▲). (a) A plot of the extent of mixing (f_m) vs square root of the annealing time ($t^{1/2}$). (b) A plot of the apparent diffusion coefficient D_{app} vs f_m.

particles, while the lower plot shows the subsequent cooling scan for these samples, from 75 to −125 °C. In these scans the position of the PBA peak for films consisting of xPBA + PBMA blends is found at the same temperature (−43 °C) and over the same range of temperatures as for a film prepared from the pure xPBA component. This indicates that there is little or no miscibility between cross-linked PBA and PBMA.

For the glass transition of the PBMA component, we find a somewhat different result (Figure 5). The maxima of the PBMA peaks in the first-derivative plot for samples with 30 and 60 vol % of xPBA moved slightly to higher temperatures (26 and 29 °C, respectively) compared with that of the pure PBMA sample (T_g = 24.5 °C), while the transition became asymmetric, with a steeper slope on the high-temperature side.

PBMA Diffusion for High-*M* PBMA Films Containing xPBA Particles. We first consider the results of MDSC experiments with the high-*M* PBMA sample itself and for its blends with 30 and 60 vol % of xPBA. In these experiments, we also observe two peaks in the first-derivative plots (not shown). Here the peaks appear at the same position and with the same shape for the individual polymers (xPBA, −43 °C; PBMA, 34 °C). Note that the T_g of the high-*M* PBMA sample is 10 °C higher than that of the low-*M* sample. These results are consistent with an absence of any substantial interaction between the two polymers at their interface.

To test the effect of the xPBA particles on the mobility of the surrounding high-*M* PBMA matrix, we examined

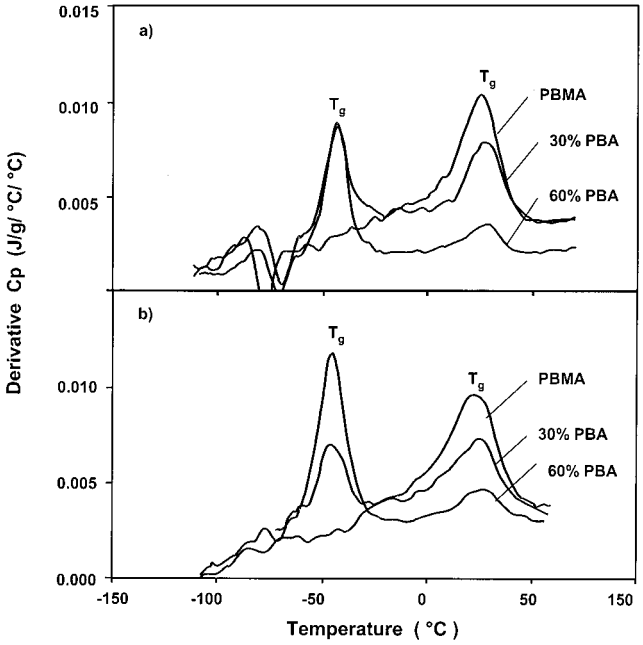

Figure 5. Plots of the first derivative of the heat capacity vs temperature for the low-*M* PBMA sample and its blends with 30 and 60 vol % of xPBA. The upper plot is the reheating scan from −125 to 75 °C, and the lower plot is the cooling scan from 75 to −125 °C.

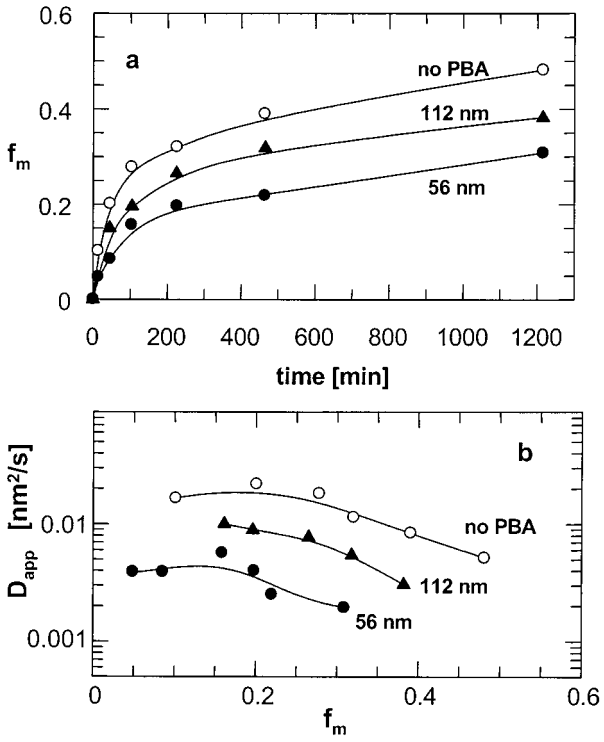

Figure 6. Comparison of high-*M* PBMA diffusion rates for pure PBMA films (○) and for films containing 30 vol % xPBA particles of different diameters (d_{xPBA}): 56 nm (●), 112 nm (▲). (a) Plots of f_m vs annealing time. (b) Plots of the apparent diffusion coefficient D_{app} vs f_m.

diffusion rates at 80 °C for the high-*M* PBMA samples under several sets of conditions. The first experiments involved films that contained 30 vol % xPBA, but with different particle diameters. Figure 6 shows the PBMA diffusion data for a pure PBMA film and for films with 30 vol % xPBA particles of different diameters, d_{xPBA} = 56 and 112 nm. The soft particles present lead to a

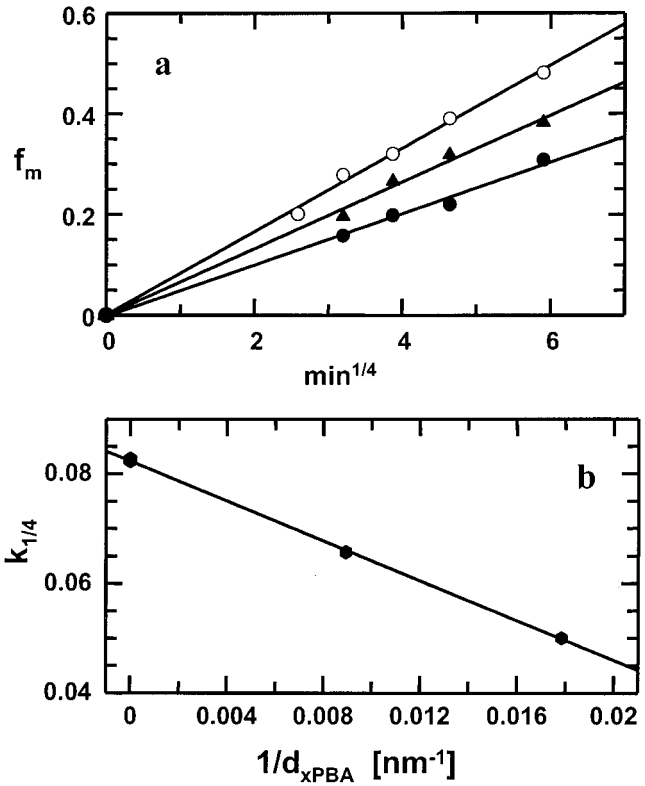

Figure 7. (a) Plots of f_m vs $t^{1/4}$ for a pure PBMA film (○) and for films containing 30 vol % xPBA particles of different diameters (d_{xPBA}): 56 nm (●) and 112 nm (▲). (b) A plot of the mobility parameter of $k_{1/4}$ (calculated from the slopes of the plots in (a)) vs $1/d_{xPBA}$ in PBMA/xPBA blend films at 30 vol % xPBA.

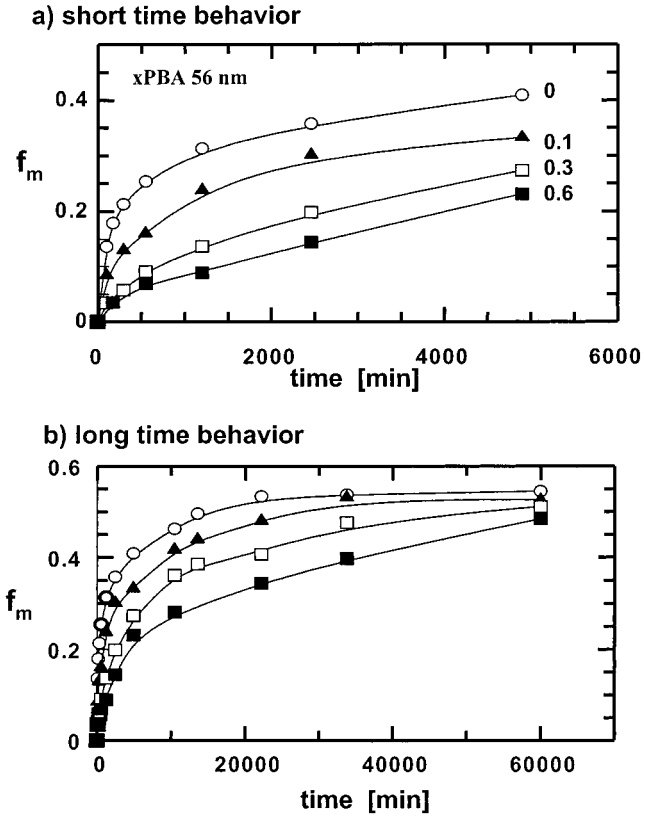

Figure 8. Plot of f_m for high-M PBMA latex containing different amounts of xPBA particles (d_{xPBA} = 56 nm), expressed as volume fraction xPBA: 0 (○), 0.1 (▲), 0.3 (□), and 0.6 (■). (a) Expanded scale, short time diffusion behavior. (b) Long time diffusion behavior.

reduction of the PBMA diffusion rate, and the xPBA particles of smaller size retard the diffusion rate to a greater extent. For an extent of mixing $f_m = 0.2$, the value of apparent diffusion coefficient D_{app} for the pure PBMA sample is 0.012 nm^2/s. This value decreases to 0.005 nm^2/s for the case of the sample with $d_{xPBA} = 112$ nm and to 0.002 nm^2/s for sample with $d_{xPBA} = 56$ nm.

Another way to compare these diffusion rates is to plot f_m as a function of $t^{1/4}$ or $t^{1/2}$, where t is the annealing time. We know from the observations described in a previous publication[22] that, for the case of high-M PBMA, f_m varies linearly with $t^{1/2}$ for $f_m \leq 0.2$ and varies linearly with $t^{1/4}$ for $f_m > 0.2$. In Figure 7a we show the results for the case where $f_m > 0.2$, where we plot f_m vs $t^{1/4}$ for the PBMA film itself and for two PBMA/xPBA blend films containing 30 vol % xPBA with different particle diameters. All three plots are linear. Because these plots are linear, we can define a mobility parameter $k_{1/4} = f_m/t^{1/4}$ characterizing each blend. On the basis of the results of Feng et al.[2] on latex films containing hard fillers, we anticipate that the changes in polymer mobility, at constant volume fraction filler, will be sensitive to the surface-to-volume ratio of the filler particles. In Figure 7b, we plot this mobility parameter against the reciprocal particle diameter ($1/d$) and obtain a straight line.

To obtain more detailed information, we carried out many more experiments at a somewhat lower temperature, 70 °C, in films containing different amounts of soft particles with a diameter, $d_{xPBA} = 56$ nm. In Figure 8b we plot f_m vs annealing time for an experiment carried out over 60 000 min (1000 h). In Figure 8a we plot the same data for the first 5000 min on an expanded scale. Figure 8 shows that the more soft filler we introduce into the film, the more the diffusion rate of PBMA decreases. Figure 8b indicates that the PBMA diffusion is not suppressed, only retarded, in the presence in the soft fillers. After a long enough time, f_m reaches the same extent of mixing as in samples without fillers.

In Figure 9a we show that the dependence of f_m on $t^{1/4}$ for $f_m > 0.2$ is linear. The mobility parameter $k_{1/4}$ decreases with an increase in the volume fraction φ of the soft filler. When we plot the mobility parameter $k_{1/4}$ vs the volume fraction of xPBA particles (Figure 9b), we observe a linear dependence (slope = −0.0213, intercept = 0.0417), excluding the point for no filler. Since all particles have the same diameter (here d = 56 nm), we infer that the parameter $k_{1/4}$ decreases in proportion to the total surface area S_{TF} of the filler particles.

In summary, we carried out two types of experiments. At constant volume fraction of the filler, we varied the diameter of the soft filler particles, and at constant filler diameter, we increased the amount of soft filler in the film. From both sets of experiments, we infer that the influence of soft filler particles on the decreasing rate of polymer diffusion in the range of $\varphi = 0.1-0.6$ depends on the total area of the filler surface. We also found that the dependence of $k_{1/4}$ on S_{TF} is linear.

In Figure 10 we show the values of f_m vs annealing time obtained at 70 °C for films containing smaller amounts of soft filler. The sample with 6 vol % xPBA shows greater retardation of polymer diffusion than the sample with 3 vol % xPBA, but for 5000 min annealing

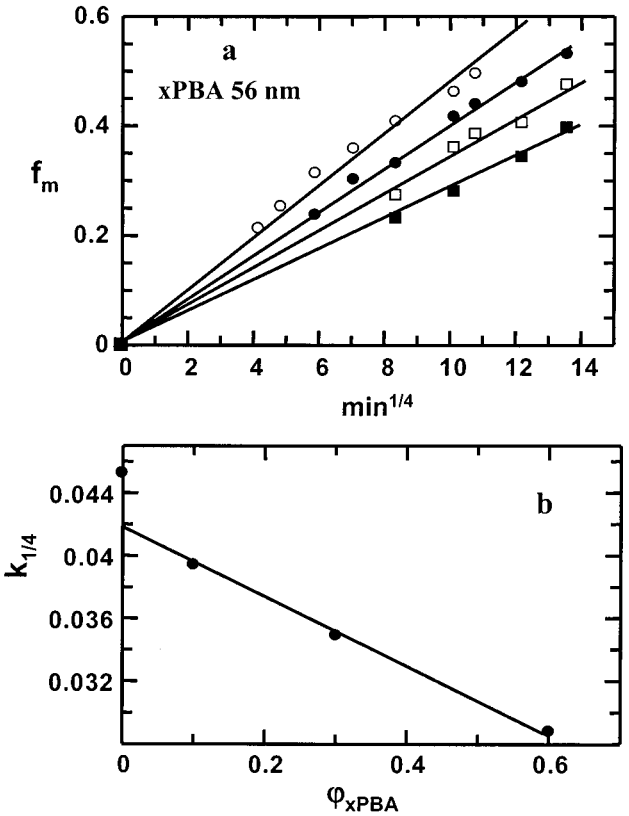

Figure 9. Plots of (a) f_m vs $t^{1/4}$ for high-*M* PBMA latex films containing different amounts of xPBA particles (d_{xPBA} = 56 nm), expressed as volume fraction xPBA: 0 (○), 0.1 (●), 0.3 (□), and 0.6 (■). (b) Plot of $k_{1/4}$ vs volume fraction xPBA.

time, the difference between the two samples disappears. In Figure 11a we plot f_m vs $t^{1/4}$, omitting the data points at 5000 min annealing time where the two lower curves in Figure 10 meet. The plots are linear. In Figure 11b, we plot the slopes, $k_{1/4} = f_m/t^{1/4}$ vs volume fraction of filler. Here we also find a linear dependence of $k_{1/4}$ on φ with a slope = −0.19 and intercept = 0.053. The slope is much steeper than that for samples with ≥10 vol % xPBA (slope = −0.021). The parameter $k_{1/4}$ for the sample without filler now falls on the line for the linear dependence presented in Figure 11b.[27]

Discussion

When a latex dispersion is allowed to dry at temperatures above the minimum film-forming temperature (MFT), one obtains a transparent film consisting of polyhedral cells formed by deformation of the latex particles. Particle deformation is driven by a combination of capillary forces associated with water evaporation and interfacial forces that oppose the formation of air voids. Under some conditions well above the polymer T_g, wet sintering can also lead to particle deformation. Routh and Russel[28] provide an up-to-date discussion of these various mechanisms. Particle deformation is resisted by the viscoelastic response of the latex polymer. For xPBA, well above its T_g, the resistance is likely associated with its elastic modulus. For PBMA, much closer to its T_g, it is the dynamic modulus that opposes deformation. The MFT can be thought of as the temperature at which the dynamic response of the polymer occurs on the same time scale as the forces associated with film drying. This temperature often corresponds to the T_g of the wet polymer.

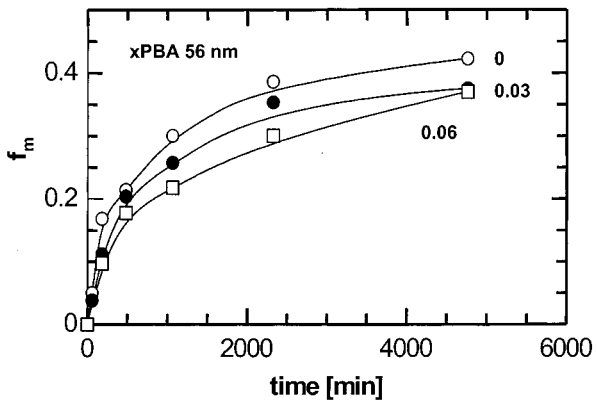

Figure 10. Plot of the extent of mixing f_m vs annealing time for high-*M* PBMA latex films containing relatively small amounts of xPBA particles (d_{xPBA} = 56 nm), expressed as volume fraction xPBA: 0 (○), 0.03 (●), 0.06 (□).

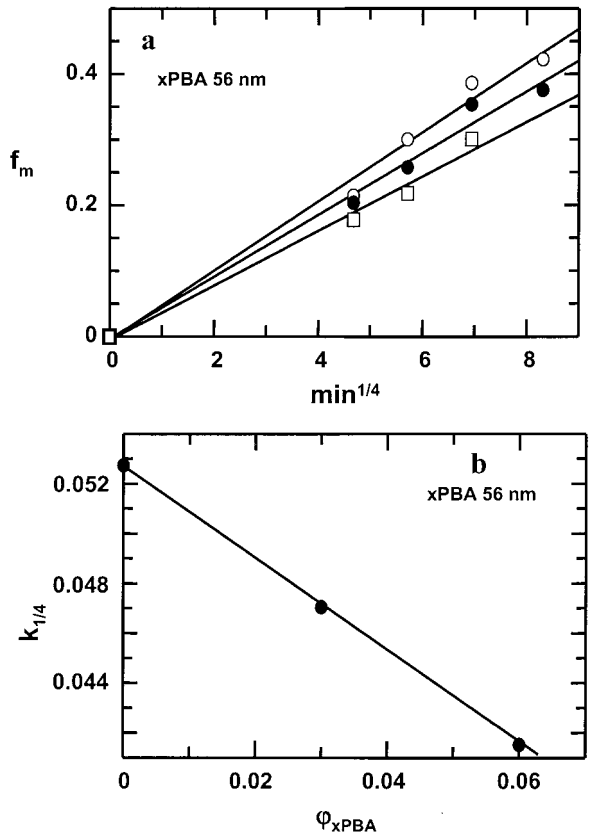

Figure 11. Plots of (a) f_m vs $t^{1/4}$ for high-*M* PBMA latex films containing small amounts of xPBA particles (d_{xPBA} = 56 nm), expressed as volume fraction xPBA: 0 (○), 0.03 (●), 0.06 (□). (b) Plot of $k_{1/4}$ vs volume fraction of filler (d_{xPBA} = 56 nm).

Newly Formed Films. Latex films prepared at temperatures just above the MFT are characterized by intimate contact between adjacent cells, in which little or no polymer diffusion has taken place.[16] Under these circumstances, as suggested in Figure 1, some energy transfer can take place across the intercellular boundaries. Since relatively few donor groups are near the boundary of the donor-labeled cells, only a small fraction of excited donors can transfer energy in this way. Previous experiments have shown that this extent of energy transfer is measurable in the case where the cells have diameters on the order of 100 nm and an extent of labeling of 1 mol %. Feng et al.[16,29] showed for hard−soft latex blends in which the hard particles were

labeled with one of the fluorescent dyes that Φ_{ET} increased in proportion to the interfacial area between hard and soft polymer in the system. Simulations show that the extent of energy transfer in such films depends on the total interfacial area between donor- and acceptor-labeled cells, multiplied by the effective thickness of the interface between the cells where some mixing of donor and acceptor groups can occur.[30] For films of the sort examined here, we expect $\Phi_{ET}(0)$ values close to 0.07 (Area(0) $\approx$ 43 ns) in the absence of filler.

In Figure 3b, we see that for films prepared from the high-*M* latex without filler we obtain results in accord with these expectations. We can conclude that no significant polymer diffusion occurs during film formation. In contrast, we see in Figure 3a that for films prepared from the low-*M* latex without filler the Area(0) value is closer to 39 ns ($\Phi_{ET}(0) = 0.22$). Since the two sets of latex particles have the same size, we anticipate the same interfacial area between donor- and acceptor-labeled cells. Thus, the difference in the extent of energy transfer must be connected to segmental or polymer diffusion during film formation, which increases the thickness of the interface between adjacent cells.

For the films prepared from the low-*M* latex, the presence of large amounts of cross-linked PBA filler particles has relatively little effect on the magnitude of $\Phi_{ET}(0)$. Area(0) values increase from 38.7 to 39.6 ns. Feng et al.[2] reported a very similar result for latex films prepared from low-*M* PBMA particles in the presence of high-T_g latex particles as hard fillers. These results imply that there is no significant change in the interfacial area between donor- and acceptor-labeled cells. Since, in filled polymers, a significant fraction of the PBMA surface area must be in contact with the unlabeled filler particles, some changes in film morphology must occur during drying to increase the area between Phe- and An-labeled polymer. One way in which this may occur is shown in the drawing I. The filler particles, shown as filled spheres, induce undulations in the boundary between Phe- and An-labeled PBMA cells, so that the presence of the filler does not affect the total interfacial area between donor- and acceptor-labeled cells.

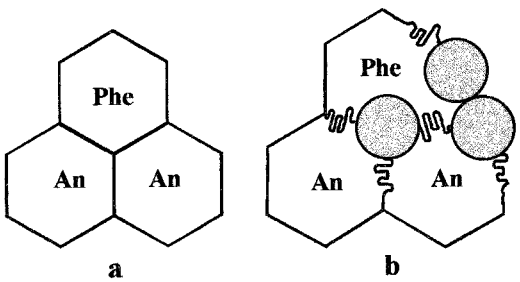

I

The results for high-*M* PBMA films with soft fillers indicate that the interfacial area between D/A labeled particles decreases with increasing volume fraction of soft particles. We would like to stress that, especially for the samples with 60% of xPBA, the Area(0) values showed significant scatter and ranged for similar samples from 43 to 45 ns. Since the unquenched lifetime of the phenanthrene chromophore in PBMA films is 45.7 ns, a value of Area(0) = 45 ns means that the donor- and acceptor-labeled PBMA particles for some samples with

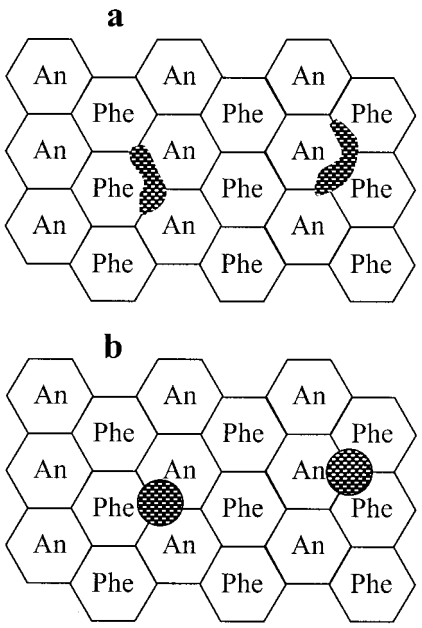

Figure 12. Schematic view of the relaxation processes in high-*M* PBMA latex films in the presence of soft cross-linked xPBA particles. (a) The morphology of the sample in the newly formed film: the xPBA particles are squeezed between the PBMA particles. (b) In the film annealed for a short period at 70 °C: when the sample is heated, the cross-linked xPBA filler particles return to their round shape. This process occurs faster than PBMA polymer diffusion in these films. We also imagine that a morphology similar to (b) is formed directly in low-*M* PBMA films containing xPBA particles.

60 vol % of xPBA were nearly completely separated by the xPBA filler particles. For these samples, however, brief annealing at 70 °C changed the area from 45 to 43 ns.

We attempt to explain these results as shown in Figure 12. For the low-*M* polymer with $T_g = 21$ °C, we imagine that, despite the low T_g of the xPBA particles ($T_g = -43$ °C), the PBMA particles themselves are easier to deform than the elastic cross-linked PBA nanospheres. Thus, the PBMA particles respond to the presence of the xPBA filler by deforming (see Figures 1 and 12b) to accommodate the spherical filler particles in much the same way they would accommodate hard filler particles. For the high-*M* polymer, with $T_g = 34$ °C, our explanation invokes the idea that it is the cross-linked PBA that flattens at the interface between adjacent PBMA latex particles. In this way they tend to form a barrier that separates donor- and acceptor-labeled cells in the newly formed film, as depicted in Figure 12a. We recall that the rate of DET decreases with the distance *r* between donor and acceptor groups as (R_0/r).[6] Since $R_0 = 2.3$ nm for the films we examine, a small increase in *r*, on the order of a nanometer, can lead to a substantial decrease in the extent of DET at that boundary. When the film is heated for short periods of time, the PBMA phase becomes more mobile. We imagine that this temperature increase has a bigger effect on the dynamic modulus of the PBMA component than on the xPBA particles, because the modulus of a polymer changes rapidly with temperature in the vicinity of its T_g. As a consequence, the flattened xPBA domains relax to their initial spherical form as indicated in Figure 12b. This increases the contact area between Phe- and An-labeled PBMA cells.

Filler Effects on Polymer Diffusion in Low-*M* Latex Films. Over the past 10 years, we have carried

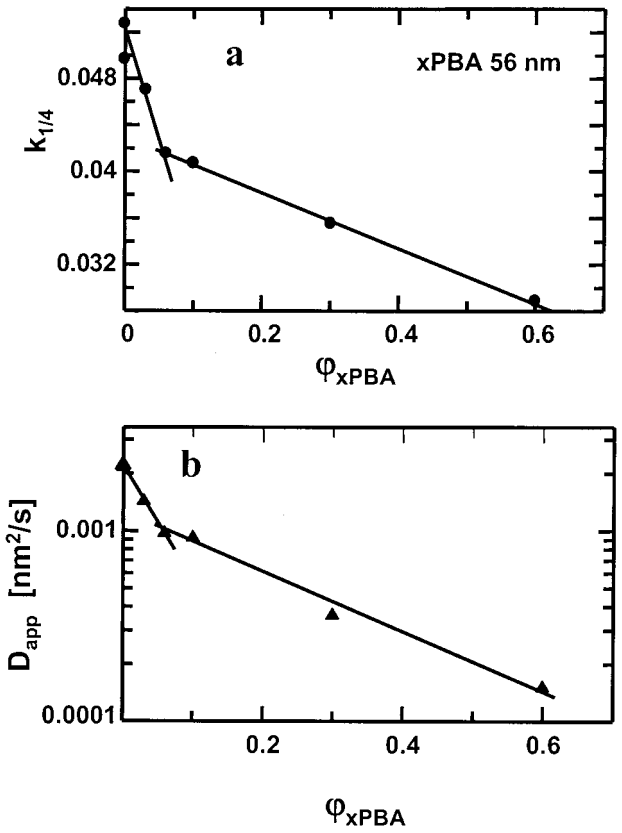

Figure 13. Plots of (a) $k_{1/4}$ vs volume fraction xPBA, where the data are taken from Figures 9b and 11b, and (b) log D_{app} vs volume fraction xPBA. The values of D_{app} refer to values at $f_m = 0.3$.

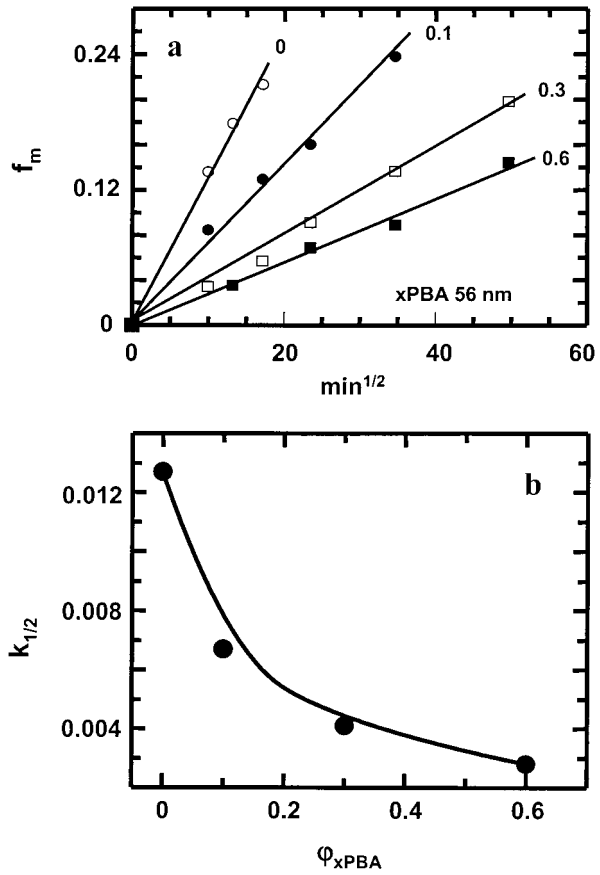

Figure 14. Plots of (a) f_m vs $t^{1/2}$ for the early time diffusion of high-M PBMA latex films containing different amounts of xPBA particles ($d_{xPBA} = 56$ nm), expressed as volume fraction xPBA: 0 (○), 10 (●), 30 (□), and 60 (■). (b) Dependence of $k_{1/2}$ on volume fraction xPBA.

out numerous studies of polymer diffusion in PBMA latex films. For all PBMA latex films we have examined in which M_w was less than twice the entanglement molecular weight, we found that f_m increased in proportion to $t^{1/2}$ up to $f_m \approx 0.7$. These results are consistent with Fickian diffusion of the polymer molecules. Similar results are shown in Figure 4. Feng et al.[2] extended these measurements to films containing high-T_g polymer nanospheres as fillers. In all of these films, they found that f_m was proportional to $t^{1/2}$, and the presence of the filler particles decreased significantly the rate of polymer diffusion. The effect is in many ways similar to that of the soft fillers in the high-M PBMA matrix to be described in more detail in the following section.

For low M PBMA in the presence of soft filler particles, we find a very different effect (Figure 4). The presence of 30 vol % xPBA particles accelerates the diffusion rate of PBMA polymer molecules in the film, whereas the presence of 60 vol % xPBA particles seems to have little effect on the PBMA diffusion rate. These results suggest that two different phenomena influence the PBMA diffusion rate in the presence of soft xPBA fillers: one that speeds up the diffusion process and another that retards diffusion. In the case of the sample with 60 vol % of xPBA, the two effects cancel.

Filler Effects on Polymer Diffusion in High-*M* Latex Films. For the high-M latex films, the polymer length (based upon M_w) is greater than 10 entanglement lengths. For these polymers, for $f_m > 0.2$, f_m increases in proportion to $t^{1/4}$ (Figures 7, 9, and 11). To proceed with the data analysis, we calculate a mobility parameter $k_{1/4} = f_m/t^{1/4}$, characterizing the rate of diffusion, as the slope in the f_m vs $t^{1/4}$ plot. Next we plot the values of the parameter $k_{1/4}$ vs $1/d_{xPBA}$ as shown in Figure 7. The linear dependence of $k_{1/4}$ on $1/d_{xPBA}$ in Figure 7 indicates that the decrease of diffusion rate is inversely proportional to the diameter of the filler particles. For spherical particles, the surface-to-volume ratio $S/V = 6/d$, where d is the diameter of the particle, so that at constant volume $S = \text{const}/d$. This result tells us that, at a given volume fraction of filler, the retardation effect increases with the total surface area of the filler particles.

We next consider the influence of the volume fraction of filler φ_{xPBA}, for particles of constant diameter, on the PBMA diffusion rate. In Figure 11, we saw that, over the range of $\varphi_{xPBA} = 0-0.06$, $k_{1/4}$ decreased linearly with an increase in φ_{xPBA}. In Figure 9, we saw a similar behavior for $0.1 \le \varphi_{xPBA} \le 0.6$, but with a smaller slope. We replot these data in Figure 13, where we observe a crossover in the range of $\varphi_{xPBA} = 0.06$. Another way to obtain information about the rate of polymer diffusion in the films is to use the f_m values to calculate apparent diffusion coefficient values D_{app}. While this calculation involves unwarranted assumptions about the nature of the diffusion process, it does provide a measure of the polymer diffusion rate. We see in Figure 13b that log D_{app} mimics the behavior of $k_{1/4}$, and a crossover in the data also appears at $\varphi_{xPBA} = 0.06$.

At early stages of polymer diffusion ($f_m < 0.2$), somewhat different results are obtained. For the samples described above, without filler and with 10, 30, and 60 vol % of xPBA particles, f_m increases linearly with $t^{1/2}$ instead of $t^{1/4}$ (Figure 14a). As in the case of the low-M

PBMA samples, we define $k_{1/2} = f_m/t^{1/2}$. The dependence of $k_{1/2}$ on the vol % of xPBA is presented in Figure 14b. This plot is not linear, indicating that at the beginning of the diffusion process the influence of soft filler on polymer diffusion is different than that during the later stages of polymer diffusion.

Mechanisms for the Change in Polymer Mobility. There are two general models commonly used to explain the change of diffusion rate in the presence of filler particles. These models differ in their description of the interactions between filler particles and the matrix. One model is based on the concept of free volume. Free volume models ascribe the change in diffusion rate to an increase (or decrease) in the microscopic friction coefficient of the diffusing species. This change is caused by the influence of the surface of the filler on the mobility of diffusing polymer in the vicinity of the filler particles through specific polymer−filler interactions. The second model is the obstacle model. Obstacles decrease the apparent diffusion rate by increasing the tortuosity of the diffusion path or by creating bottlenecks for diffusion, without affecting the friction experienced by the diffusing species. A change in free volume can lead to an increase or a decrease in the rate of polymer diffusion, whereas the presence of obstacles always leads to a decrease in the polymer diffusion rate.

We speculate that there may be a slight miscibility of low-*M* PBMA with xPBA in the matrix. A diffuse interface between these components may lead to an increase in free volume, which in turn gives rise to an increase in the rate of diffusion of the PBMA molecules in the film.[31] Opposing this effect are the obstacles created by the PBMA nanoparticles in the film. The magnitude of the obstacle effect increases with the number of obstacles. For the low-*M* PBMA sample containing 60 vol % xPBA, the two effects cancel.

Obstacle effects can operate in two different ways in our system, as shown in the drawing **II**, where the filler particles are shown in gray. PBMA molecules forced to diffuse around individual filler particles as in **b** follow a longer pathway. Polymer molecules forced to diffuse through a bottleneck as shown in **a** can experience an additional entropic barrier if the dimensions of the bottleneck are the size of, or smaller than, the radius of gyration of the diffusing PBMA molecules.

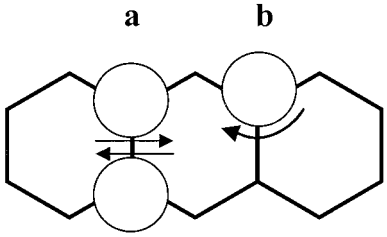

II

Film Morphology. The morphology of a film formed from a blend of two types of latex particles is determined in the aqueous phase as the dispersion dries. If the two types of particles are randomly distributed in the fluid phase and retain their random distribution as the dispersion becomes more concentrated, then the dry film will consist of a random distribution of the different types of particles. If, however, phase separation occurs in the fluid phase, then the structures formed in solution will carry forward into the film. For example, in mixtures of large and small particles, there is a tendency for the small particles to fill the interstitial spaces between the large particles, forming percolation networks in the dry film. Depending upon the nature of the blend, this type of morphology has been inferred from measurements of the macroscopic properties of the dry latex films, such as the conductivity (in blends containing conductive fillers),[32] the elastic modulus,[33] or the tensile modulus[1a] of the film.

Eckersley and Helmer[34] examined a series of latex films prepared from a mixture of hard and soft latex particles of different sizes. They showed that the presence of small hard particles in the soft polymer matrix led to a substantial increase in the film modulus and tensile strength. The magnitude of the effect depended not only on the composition of the film but also on the ratio of the particle diameters. The smaller the filler diameter, the less is needed to form a continuous phase in the film.

Chevalier et al.[33] examined particle aggregation in latex blend films by dynamic mechanical analysis (DMA)[35] and by small-angle neutron scattering (SANS).[36,37] These two experimental methods give complementary information about the morphology of latex films by providing structural information on very different length scales. Chevalier et at.[33] examined the structure of composite films consisting of high-T_g polystyrene (PS) latex particles dispersed in a low-T_g poly(butyl acrylate) latex film. For the SANS experiments, they investigated samples with two filler concentrations: 10 and 45 wt % PS. The most important experimental result was that the position and shape of the scattering peak was identical for both samples, indicating that the local morphology of the films at the two different PS particle concentrations is the same. From SANS experiments, they found that the PS particles were not randomly distributed in the PBA film. The mean separation between PS particles was shorter than that expected for a random distribution, indicating that PS particles were aggregated into relatively open clusters. They inferred that the film consisted of regions that were enriched in PS particles, at the expense of the remaining regions containing fewer PS particles than the average. The composition of the PS-rich domains (60 vol % PS) was similar, regardless of the overall composition of the film. This type of behavior resembles features of phase separation where the separate phases do not consist of pure components.

From the DMA measurements of the elastic moduli G' (sensitive to the large-scale structure topology arrangement of the hard particles),[33] the authors found that the percolation threshold, connected with efficient mechanical reinforcement of the film, occurred at 32 wt % PS. DMA measurements, however, were not sensitive to the formation of PS clusters below the percolation threshold. The influence of the aggregates on mechanical properties was manifested only above the percolation threshold. On the other hand, the SANS experiment was not able to detect the formation of a continuous PS network in the film but was sensitive to the formation of local structure in the form of PS clusters present at 10 vol % PS.

Local Morphology in Latex Blend Films. The energy transfer experiments described in this paper provide results that are sensitive to the local morphology of the latex blend films, but the inferences one can draw from them are limited. We had hoped to be able to

determine this morphology directly through transmission electron microscopy (TEM) measurements, particularly freeze-fracture TEM measurements. These experiments proved to be unexpectedly difficult.[38] To guide future microscopy experiments, we consider ways in which the morphology of the blend might lead to the behavior we observed, both for the case of newly formed films and for retarded PBMA diffusion rates in films subjected to annealing. While these explanations are speculative, we prefer to think of them as hypotheses, which we hope can be tested in future experiments.

In experiments carried out on newly formed high-*M* PBMA latex films, we found that the presence of xPBA particles led to a decrease in the quantum efficiency of intercellular energy transfer, compared to filler-free latex films. Brief heating to 70 °C followed by cooling to room temperature led to an increase in Φ_{ET}. From these results we deduced that the soft elastic xPBA particles deform under the capillary forces accompanying drying of the dispersion. In Figure 12a we picture them as pancakelike objects that act to separate Phe- and An-labeled cells. Upon heating, the dynamic modulus of the PMBA decreases to a much greater extent than the modulus of the cross-linked PBA, and the xPBA particles relax to recover their spherical shape (Figure 12b). This change in morphology is accompanied by an increase in the contact area between Phe- and An-labeled cells.

In annealing experiments carried out on films prepared from blends of xPBA with high-*M* PBMA, we observed that the presence of the soft filler led to a significant retardation in the diffusion rate of the PBMA component. Before we can hypothesize how this retardation may arise, we need to understand an important feature of the DET experiment itself. The experiments we carry out measure the extent of polymer diffusion over relatively short distances. For DET experiments in latex films, f_m approaches unity as the mean diffusion distance approaches that of a particle radius (60 nm).[39] Polymer diffusion over larger distances no longer contributes to a change in the DET signal. Under these circumstances, obstacle effects are manifest only as they influence the short-range diffusion of the PBMA molecules in the latex film. The nature of this influence must depend in a sensitive way on the morphology of the latex films containing the two components, xPBA and PBMA.

All of the experiments we carried out indicate that the rate of polymer diffusion of the PBMA molecules decreases in proportion to the increase in surface area of the xPBA filler particles present in the matrix. For constant φ_{xPBA}, $k_{1/4}$ decreases as $1/d$, and for constant d, $k_{1/4}$ decreases linearly with increasing φ_{xPBA}. Since the effect of each particle introduced into the matrix appears to be independent and additive, the film itself must have a morphology in which the distribution of filler particles has a rather open structure. If the filler particles formed dense spherical aggregates, for example, the surface area of the aggregate would increase only $n^{2/3}$, where n is the number of xPBA particles in the aggregate. Under these circumstances, $k_{1/4}$ would not decrease linearly φ_{xPBA}.

Somewhat deeper insights into the film morphology are possible, based upon the crossover seen in the plot in Figure 13. The steep slope observed at low filler particle densities suggests that under these circumstances the filler particles are isolated in the film and that the entire surface area of the particles contributes to the retardation of the diffusion of the PBMA molecules in the vicinity of the filler. From this point of view, the crossover corresponds to the onset of aggregation of filler particles. We envision open aggregates, which may or may not at this point span the film. In other words, the DET experiment may be sensitive to the onset of aggregation below the percolation threshold. This is an idea that can be tested in future experiments by dynamic mechanical measurements on the film.

Summary

The presence of soft, elastic particles in high-*M* PBMA latex films strongly decreases the diffusion rate of the PBMA molecules across the intercellular boundaries. The retardation effect depends on the total surface area of filler particles being in contact with diffusing polymer and is best explained as an obstacle effect on PBMA diffusion. Very different results are found for the low-*M* PBMA sample, where the presence of 30 vol % cross-linked PBA particles increases the diffusion rate of the PBMA polymer. In the presence of 60 vol % cross-linked PBA particles, the PBMA diffusion rate is the same as that in the latex film without filler. Thus, the overall effect of soft filler particles on polymer diffusion is a combination of an obstacle effect, which retards polymer diffusion, and a second effect, probably a free volume effect, which promotes polymer diffusion. We imagine that the free volume effect arises as a consequence of, or is enhanced by, a slight miscibility of segments of the cross-linked PBA filler particles with the low-*M* PBMA polymer. This effect is much smaller for the high-*M* PBMA sample. Depending on which of these effects dominates, one can observe an increase or decrease in the polymer diffusion rate.

Acknowledgment. The authors thank ICI, ICI Canada, and NSERC Canada for their support of this research. We also thank E. Meyer at the ICI Paints laboratory in Strongsville, OH, for the use of their DSC apparatus.

References and Notes

(1) (a) Hsu, W. H.; Wu, S. *Polym. Eng. Sci.* **1993**, *33*, 293. (b) Tsagaropolous, G.; Eisenberg, A. *Macromolecules* **1995**, *28*, 6067. (c) Vollenberg, P.; Heinkens, D. *Polymer* **1989**, *30*, 1659. (d) Lucis, S.; Kovacevic, V.; Hace, D. *Int. J. Adhes. Adhes.* **1998**, *18*, 115.
(2) Feng, J.; Odrobina, E.; Winnik, M. A. *Macromolecules* **1998**, *31*, 5290.
(3) Lipatov, Y. S.; Sergeeva, L. M. *Adsorption of Polymers*; Wiley: New York, 1974. Bitsanis, I.; Hadziioannou, G. *J. Chem. Phys.* **1990**, *92*, 3827. Baschnagel, J.; Binder, K. *Macromolecules* **1995**, *28*, 6808. Baschnagel, J.; Binder, K. *J. Phys. I* **1996**, *6*, 1271. Brown, H. R.; Russell, T. P. *Macromolecules* **1996**, *29*, 798.
(4) Mansfield, K. F.; Theodorou, D. N. *Macromolecules* **1991**, *24*, 6283.
(5) Mayes, A. M. *Macromolecules* **1994**, *27*, 3114.
(6) Honeycutt, J. D.; Thirumalai, D.; Klimov, D. K. *J. Phys. A: Math. Gen.* **1989**, *22*, L169.
(7) Frank, B.; Gast, A. P.; Russell, T. P.; Brown, H. R.; Hawker, C. *Macromolecules* **1996**, *29*, 6531.
(8) Zheng, X.; Rafailovich, M. H.; Sokolov, J.; Strzhemechny, Y.; Schwarz, S. A.; Sauer, B. B.; Rubinstein, M. *Phys. Rev. Lett.* **1997**, *79*, 241.
(9) Lin, E. K.; Wu, W. L.; Satija, S. K. *Macromolecules* **1997**, *30*, 7224.
(10) Orts, W. L.; van Zanten, J. H.; Wu, W. L.; Satija, S. K. *Phys. Rev. Lett.* **1993**, *71*, 867.
(11) Keddie, J. L.; Jones, R. A. L.; Cory, R. R. *Europhys. Lett.* **1994**, *27*, 59.

(12) Reiter, G. *Macromolecules* **1994**, *27*, 3046.
(13) Forrest, J. A.; Dalnoki-Verres, K.; Dutcher, J. R. *Phys. Rev. Lett.* **1996**, *77*, 2002.
(14) Forrest, J. A.; Dalnoki-Verres, K.; Dutcher, J. R. *Phys. Rev. E* **1997**, *56*, 5705.
(15) Long, D.; Lequeue, F. *Eur. Phys. J. E* **2001**, *4*, 371.
(16) Feng, J. Ph.D. Thesis, University of Toronto, 1997.
(17) Feng, J.; Winnik, M. A. *Macromolecules* **1997**, *30*, 4324.
(18) O'Connor, D. V.; Phillips, D. *Time-Correlated Single Photon Counting*; Academic Press: London, 1984.
(19) Berlman, I. B. *Energy Transfer Parameters of Aromatic Compounds*; Academic Press: New York, 1973.
(20) Briber, R. M.; Liu, X.; Bauer, B. J. *Science* **1995**, *268*, 395.
(21) Farinha, J. P. S.; Martinho, J. M. G.; Yekta, A.; Winnik, M. A. *Macromolecules* **1995**, *28*, 6084.
(22) Odrobina, E.; Winnik, M. A. *Macromolecules* **2001**, *34*, 6029.
(23) Dhinojwala, A.; Torkelson, J. M. *Macromolecules* **1994**, *27*, 4817. Liu, Y. S.; Feng, J.; Winnik, M. A. *J. Chem. Phys.* **1994**, *101*, 9096. Kim, H.-B.; Winnik, M. A. *Macromolecules* **1995**, *28*, 2033.
(24) (a)Yekta, A.; Duhamel, J.; Winnik, M. A. *Chem. Phys. Lett.* **1995**, *235*, 119. (b) Farinha, J.; Martinho, J. M. G.; Yekta, A.; Winnik, M. A. *Macromolecules* **1995**, *28*, 6084.
(25) Crank, J. *The Mathematics of Diffusion*; Clarendon: Oxford, 1974.
(26) Kim, H.-B.; Winnik, M. A. *Macromolecules* **1994**, *27*, 1007.
(27) The experiments at 70 °C with 0, 3, and 6 vol % xPBA were carried out separately from those with 0 and 10 vol % xPBA. Since a small change in oven temperature can have large effect on the polymer diffusion rate, we tested for this possibility by comparing the two plots of f_m vs t for the samples without filler. These were identical.
(28) Routh, A. F.; Russel, W. B. *AIChE J.* **1998**, *44*, 2088; *Langmuir* **1999**, *15*, 7762.
(29) Feng, J.; Yekta, A.; Winnik, M. A. *Chem. Phys. Lett.* **1996**, *260*, 296.
(30) Farinha, J. P. S.; Vorobyova, O.; Winnik, M. A. *Macromolecules* **2000**, *33*, 5863.
(31) This speculation about partial miscibility between xPBA and low-*M* PBMA is not supported by the DSC experiments, which show a slight shift to higher T_g for the low-*M* PBMA component in the presence of xPBA (Figure 5).
(32) Wang, Y.; Anderson, Ch. *Macromolecules* **1999**, *32*, 6172.
(33) Chevalier, Y.; Hidalgo, M.; Cavaillé, J. Y.; Cabane, B. *Macromolecules* **1999**, *32*, 7887.
(34) Eckersley, S. T.; Helmer, B. J. *J. Coat. Technol.* **1997**, *69* (864), 97.
(35) (a) Cavaillé, J.-Y.; Pérez, J. *Macromol. Chem., Macromol. Symp.* **1990**, *35/36*, 405. (b) Cavaillé, J.-Y.; Vassoille, R.; Thollet, G.; Rios, L.; Pichot, C. *Colloid Polym. Sci.* **1991**, *269*, 248. (c) Ouali, N.; Cavaillé, J.-Y.; Pérez, J. *Plast., Rubber Compos. Process. Appl.* **1991**, *16*, 55. (d) Favier, V.; Chanzy, H.; Cavaillé, J.-Y. *Macromolecules* **1995**, *28*, 6365.
(36) *Neutron, X-ray and Light Scattering: Introduction to an Investigative Tool for Colloidal and Polymeric Systems*; Linder, P., Zemb, Th., Eds.; North-Holland: Amsterdam, 1991.
(37) Chevalier, Y. *Trends Polym. Sci.* **1996**, *4*, 197.
(38) Film samples were fractured at −170 °C and coated with a thin Pt/C mask. For PBMA films, the polymer could be removed from the mask with organic solvents such as chloroform. Beautiful images were obtained from TEM measurements on the Pt/C masks. For xPBA−PBMA blend films, we had great difficulty removing the cross-linked xPBA portions from the mask. The polymer remaining on the mask created shadows in the TEM that obscured the images.
(39) (a) Farinha, J. P. S.; Martinho, J. M. G.; Yekta, A.; Winnik, M. A. *Macromolecules* **1995**, *28*, 6084. (b) Farinha, J. P. S.; Martinho, J. M. G.; Kawaguchi, S.; Winnik, M. A. *J. Phys. Chem.* **1996**, *100*, 12552.

MA002052E